Current Biology, Volume *23*

Supplemental Information

Keratocyte Fragments and Cells Utilize Competing Pathways to Move in Opposite Directions in an Electric Field

Yaohui Sun, Hao Do, Jing Gao, Ren Zhao, Min Zhao, and Alex Mogilner

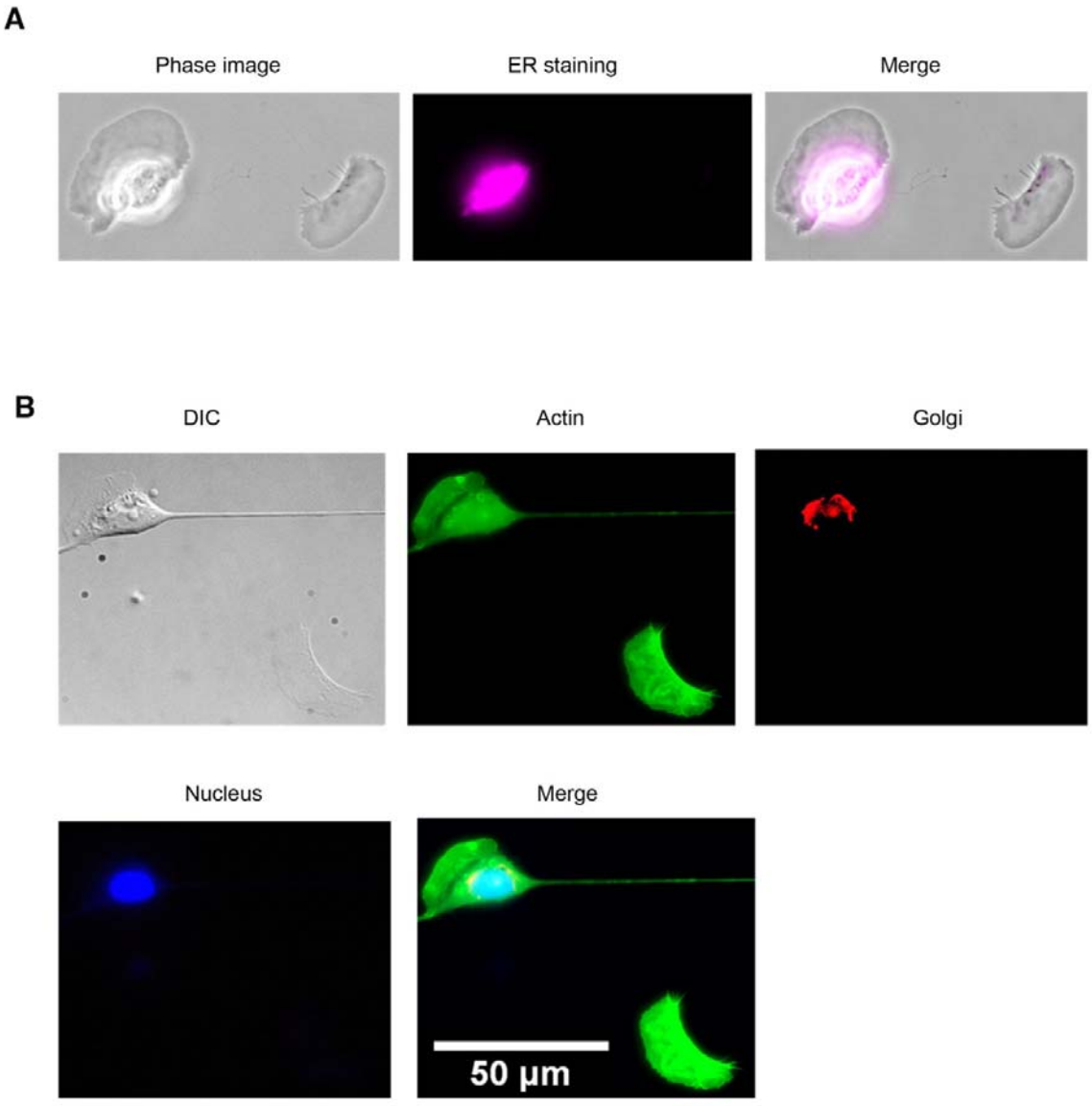

Figure S1. Fragments lack Nucleus, Endoplasmic Reticulum and Golgi, Related to Figure 3
(A) Images for keratocyte and fragment in phase contrast (left panel), with labeled ER (Middle panel in magenta) and merged (right panel). Note: there were fragments with no ER at all;

however, a number of fragments displayed some stain with the ER tracker that was much weaker than that displayed by the whole cells.
(B) Images for keratocyte and fragment in DIC (upper left panel), with labeled actin (green), Golgi (red), counterstained nuclei (blue) and merged (lower right panel). Scale bar equals 50 μm.

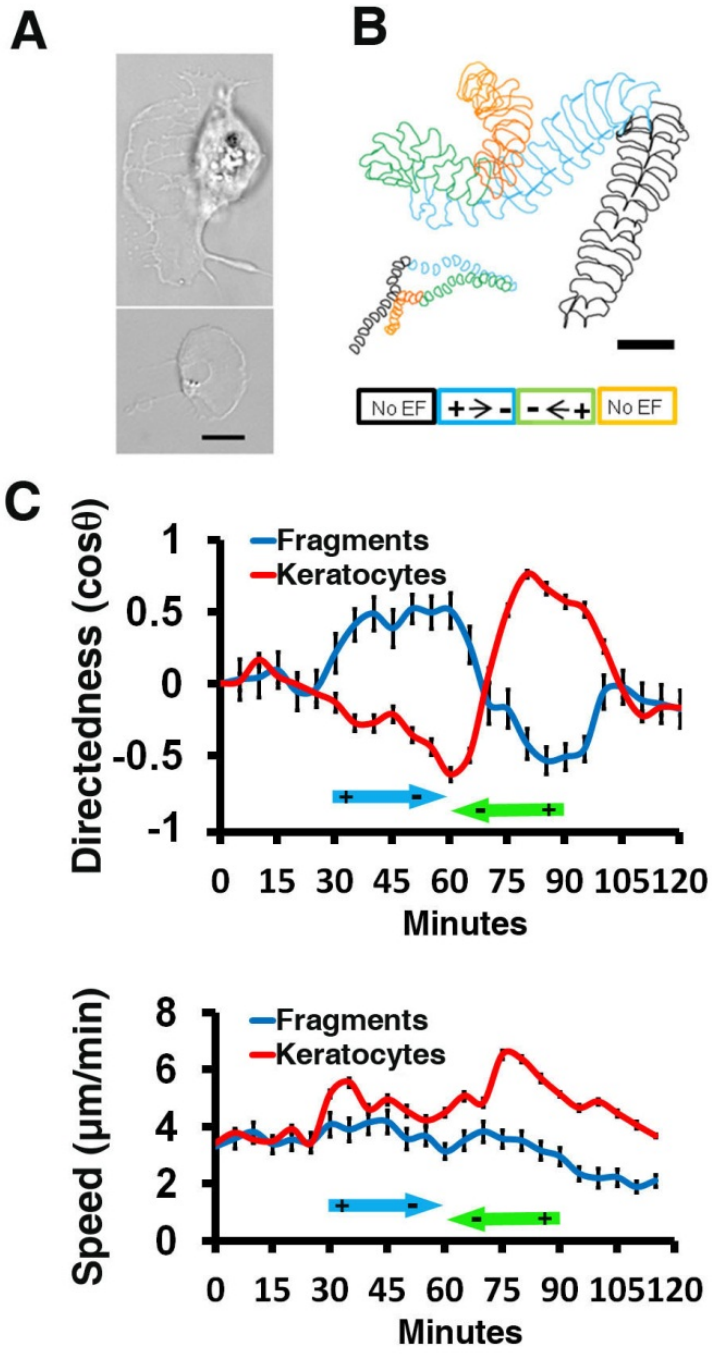

Figure S2. **Both cells and fragments respond rapidly to the EF direction switch, Related to Figure 1**

(A) DIC images of representative keratocyte (top panel) and fragment (bottom panel) generated with Staurosporin treatment. Scale bar equals 5 μm.

(B) Contour overlays of the cell and fragment shown in (A) during a 120 minute time course. EF polarity (4 V/cm) is color coded. Scale bar equals 50 μm.

(C) Directedness and trajectory speed of keratocytes (n = 13) and fragments (n = 32) as functions of time with 5 minute increments. EF polarity (4 V/cm) is color coded.

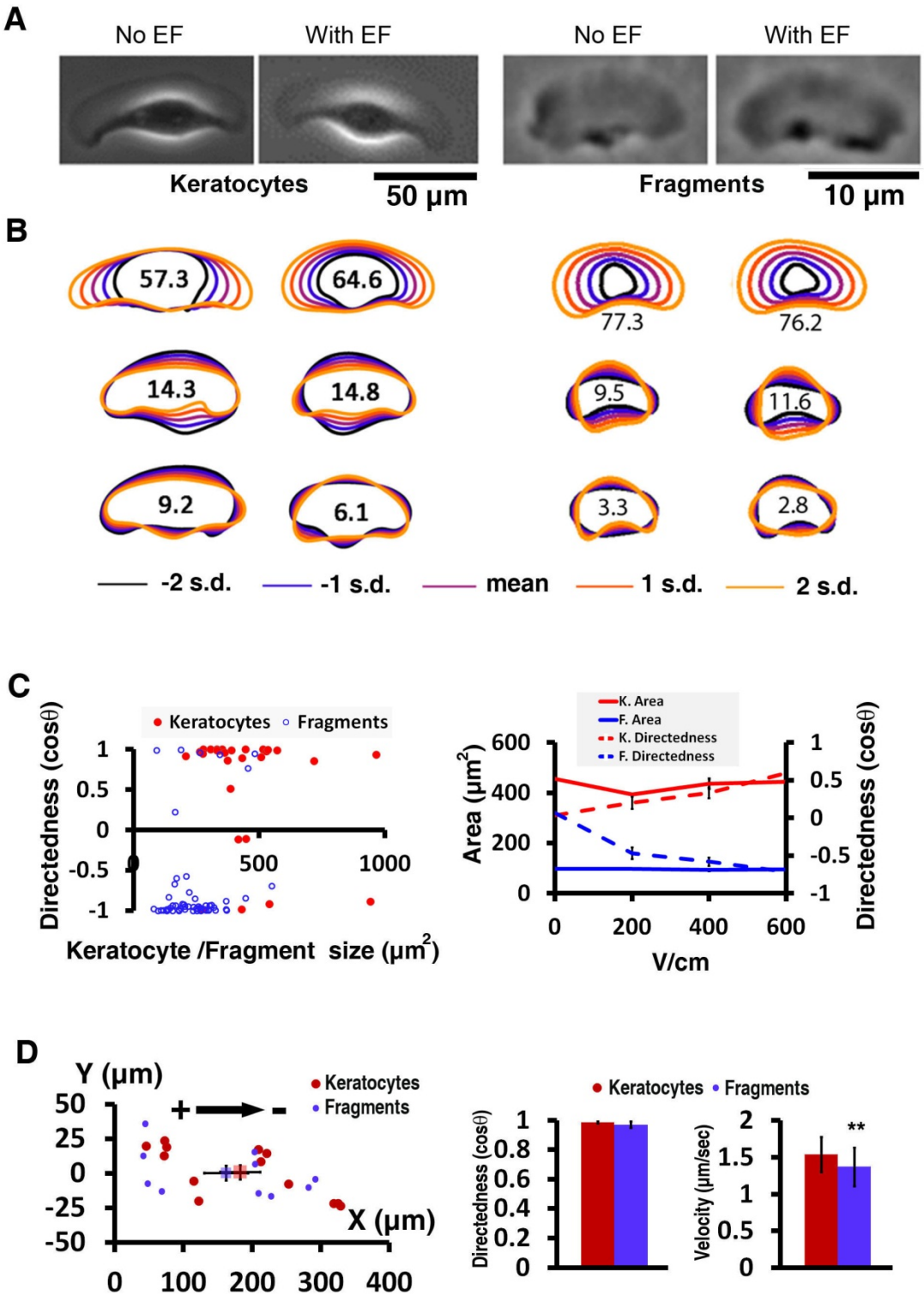

Figure S3. Galvanotaxis of cells and fragments is size- and shape-independent, Related to Figure 4

(A) Phase contrast images of representative keratocytes (left panels) and fragments (right panels) with and without EF exposure.

(B) Shapes of cells and fragments are not affected significantly by EF: Principal modes of shape variation of keratocytes (left panels) and fragments (right panels) with or without EF exposure, as determined by principal component analysis of aligned cell outlines. For each population of cells, the mean keratocyte/fragment shape and shapes one and two standard deviations from the mean are shown for each shape mode. The variation accounted for by each mode is indicated.
(C) Left: Scatter plots show directedness as a function of the size of keratocyte (red) and fragment (blue). The areas (μm^2) of keratocytes or fragments exposed to an EF of 6 V/cm for 30 minutes were measured and used for correlation analysis. Correlation coefficient is less than 0.2. Right: Directedness (dashed lines) of keratocyte cells and fragments is voltage dependent but size independent. No correlation between directedness and average area (solid lines) of keratocyte/fragment under different EF strength could be drawn.
(D) Electrophoretic properties of keratocyte (red, n = 13) and fragment (blue, n = 10). Scatter plot of the end point coordinates of keratocytes and fragments in suspension when exposed to an EF of 4 V/cm for 2 minutes (left panel). Squares represent the average values for each population; error bars indicate standard error of the mean. EF vector is marked by +/– and its orientation is indicated by arrow. Under EF strength of 4 V/cm, both keratocytes and fragments move with nearly maximal directionality to the cathode (middle panel). Fragments migrate slightly slower than keratocytes (right panel, **: $p < 0.01$).

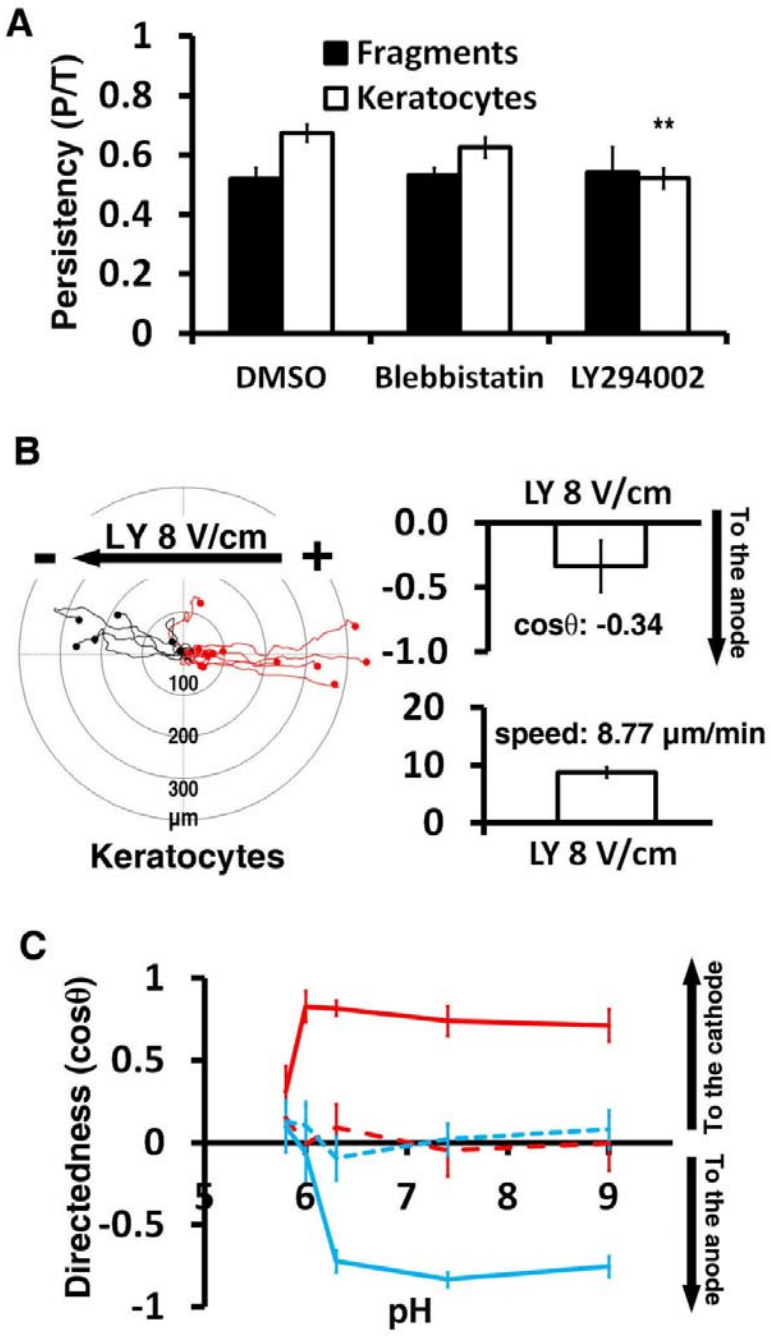

Figure S4. Effects of PI3K and myosin inhibition and pH level on cells' and fragments' persistency and directedness in EF, Related to Figure 2

(A) Keratocytes and fragments were treated with Blebbistatin (50 μM) or LY294002 (50 μM). Images were taken every 30 seconds. Migration persistency is calculated by displacement distance / trajectory distance after cells or fragments travelled for 30 minutes. Decreased migration persistency was observed in keratocytes but not fragments in the presence of PI3K inhibitor. ** ($p < 0.01$) indicates that the difference between DMSO and LY294002 is significant.

(B) Left: Trajectories of keratocytes in the presence of LY294002 when exposed to an EF of 8 V/cm. Total of 18 cells were traced. 12 were directed to the anode (red) while 6 to the cathode (black). Note that one cell originally migrating to the cathode underwent direction switching. Right: Quantification of directionality (top) and speed (bottom) of keratocytes (n=18) in the presence of LY294002 (50 μM). EF = 8 V/cm. Duration: 30 minutes.
(C) Directedness of keratocytes (red) and fragments (blue) in EF (solid lines) as functions of pH compared to the controls in the absence of an EF (dotted lines).

Table S1. Summary of directionality and speed of keratocytes and fragments exposed to EF under various conditions, Related to Figure 2

Condition/Voltage (V/cm)		Keratocytes			Fragments		
		N	Directedness (cosθ) Mean ± SE	Speed (μm/min) Mean ± SE	N	Directedness (cosθ) Mean ± SE	Speed (μm/min) Mean ± SE
	0.0	53	0.06 ± 0.05	6.16 ± 0.21	40	-0.13 ± 0.05	4.73 ± 0.21
	0.1	47	-0.01 ± 0.11	3.79 ± 0.24	47	-0.04 ± 0.11	5.32 ± 0.39
	0.2	47	0.18 ± 0.10	3.30 ± 0.21	60	0.12 ± 0.10	2.74 ± 0.23
	0.5	53	0.06 ± 0.09	5.78 ± 0.48	61	-0.28 ± 0.08	4.65 ± 0.29
	1.0	32	0.14 ± 0.08	5.71 ± 0.43	53	-0.22 ± 0.11	4.73 ± 0.34
	2.0	51	0.20 ± 0.08	7.16 ± 0.42	50	-0.47 ± 0.08	3.24 ± 0.17
	4.0	24	0.81 ± 0.07	8.26 ± 0.74	30	-0.65 ± 0.12	3.40 ± 0.56
	6.0	39	0.77 ± 0.05	7.03 ± 0.31	151	-0.59 ± 0.05	3.43 ± 0.13
DMSO	4.0	52	0.65 ± 0.06	11.11 ± 0.59	54	-0.66 ± 0.08	4.99 ± 0.42
LY294002	4.0	52	0.08 ± 0.11	5.62 ± 0.28	21	-0.45 ± 0.23	5.45 ± 0.75
Blebbistatin	4.0	51	0.82 ± 0.06	9.39 ± 0.39	57	-0.15 ± 0.11	7.60 ± 0.47
LY+BB	4.0	34	0.06 ± 0.13	7.58 ± 0.64	30	-0.14 ± 0.13	9.25 ± 0.89
Y27632	4.0	32	0.47 ± 0.11	5.39 ± 0.34	55	-0.22 ± 0.09	5.65 ± 0.25
CK-666	4.0	22	0.83 ± 0.07	4.84 ± 0.30	22	-0.23 ± 0.15	4.16 ± 0.26
EGTA	4.0	30	0.82 ± 0.03	3.87 ± 0.18	41	-0.10 ± 0.12	2.60 ± 0.15
Nocodazole	4.0	54	0.45 ± 0.10	9.73 ± 0.47	52	-0.42 ± 0.09	6.40 ± 0.35
pH 5.8	4.0	22	0.31 ± 0.16	0.01 ± 0.46	27	0.10 ± 0.13	0.01 ± 0.75
pH 6.0	4.0	21	0.83 ± 0.10	3.15 ± 0.22	17	-0.06 ± 0.20	3.08 ± 0.34
pH 6.3	4.0	30	0.82 ± 0.04	11.63 ± 0.54	30	-0.72 ± 0.07	8.23 ± 0.40
pH 7.4	4.0	27	0.74 ± 0.09	12.98 ± 1.14	44	-0.83 ± 0.04	8.25 ± 0.64
pH 9.0	4.0	16	0.71 ± 0.10	5.81 ± 0.39	34	-0.75 ± 0.06	5.49 ± 0.39

Data from a representative experiment.
Directedness is calculated as cosine angle between lines of displacement and electric field vector 30 minutes after the exposure. Positive: moving to cathode. Negative: moving to anode.
Drugs were applied as described in Experimental Procedures.
pH was adjusted as described in Experimental Procedures.

SUPPLEMENTAL EXPERIMENTAL PROCEDURES

The Institutional Animal Use and Care Committees of the University of California at Davis approved the animal procedures used in this study (protocol number is 16478), which were performed in accordance with NIH guidelines.

Keratocyte isolation and fragment induction: Scales were removed from the flanks of black skirt tetra *Gymnocorymbus ternetzi* and allowed to adhere to the bottom of a culture dish. The scales were covered by a glass 22-mm coverslip with a stainless steel nut on the top to hold the scales in position, and cultured at room temperature in Leibovitz's L-15 media (Gibco BRL), supplemented with 14.2 mM HEPES pH 7.4, 10% Fetal Bovine Serum (Invitrogen), and 1% antibiotic-antimycotic (Gibco BRL). Sheets of keratocytes that migrate off the scale after 24-48 hours were dissociated by a brief treatment with 0.25% Trypsin/0.02 EDTA solution (Invitrogen) in phosphate buffered saline (PBS). Isolated keratocytes were seeded in tissue culture dish and incubated at room temperature for 1-3 hours to allow attachment. Cell fragment formation was induced by 100 nM staurosporine (Sigma) in culture media at 35°C for 30 min with the lid half open. Cells and fragments are washed in normal media and allowed to recover for at least 10 min before observation on the microscope [1].

EF application and time-lapse recording: The electrotaxis experiments were carried out as previously described [2-4] in custom-made electrotaxis chambers (20 mm x 10 mm x 0.1 mm). The chambers were built over tissue culture treated dishes. These custom-made electrotaxis chambers with small cross-sectional area provided high resistance to current flow and minimized Joule heating during the experiment. To eliminate toxic products from the electrodes that might be harmful to cells, agar salt bridges made with 1% agar gel in Steinberg's salt solution were used to connect silver/silver chloride electrodes in beakers of Steinberg's salt solution to pools of excess medium at either side of the chamber.

Cell migration was recorded with a Zeiss Axiovert 40 with a Hamamatsu C4742-95 CCD digital camera (Hamamatsu Corporation) attached. Time-lapse experiments were performed using a SimplePCI 5.3 imaging system with a motorized X, Y, Z stage (BioPoint 2, Ludl Electronic Products Ltd.). Typically in each experiment, 4-6 fields under low magnification of 10x were chosen. Images were taken at 30 second intervals at room temperature. Each experiment lasted up to 2 hours. Drugs (all purchased from Sigma) were added in the medium in the following concentration: DMSO (0.1%), LY294002 (50 μM), Blebbistatin (50 μM), Y27632 (10 μM), EGTA (5 mM), Nocodazole (10 μM), CK-666 (100 μM). To adjust the pH in Leibowitz-15 media with 10% fetal bovine serum we titrate the media with 15 mM of appropriate buffers. For media with a pH of 5.8, 6.0, or 6.2, MES buffer was used. For media with a pH of 7.4, HEPES buffer was used. For media with a pH of 9, Tris buffer was used. [5]. In the case of electrophoretic experiment, keratocytes and fragments were released with trypsin/EDTA, washed once with normal medium and seeded in electrotaxis chamber. Time-lapse recording was processed immediately before cellular attachment to the surface.

Data processing and quantification: Time-lapse images were imported into ImageJ (http://rsbweb.nih.gov/ij). Tracks were marked by using the MtrackJ tool and plotted by using the Chemotaxis tool. Two parameters of cell migration were quantified: 1) Directedness, a

measurement to quantify how directionally cells migrated in response to EFs [6]. The angle that each cell moved with respect to the EF vector was measured and its cosine value was calculated as directedness [7]. If a cell moved perfectly along the field vector toward to cathode, the cosine of this angle would be 1; if the cell moved perpendicularly to the field vector the cosine of this angle would be 0; and -1 if the cell moved directly toward to anode. 2) Trajectory speed, which is used to define the migration rate, is the distance (in μm) traveled by the cell over sixty-second interval divided by this time interval (during this interval, cells and fragments turn little, so this measurement introduces but a small error). To measure the cell size, the initial two dimensional areas of keratocytes and fragments right before EF application were calculated in ImageJ.

Contour overlay and principal component analysis: Phase contrast images of keratocytes or fragments were converted into the binary images using custom written Matlab code (Script available upon request). Briefly, we used Matlab edge detection and a basic morphology function to outline the cells/fragments in the phase contrast image. We use the Otsu method [8] to erase the halo artifacts. If shape was still unsatisfactory, we then used the Lasso tool in Photoshop (Adobe) to manually extract the cell shape. Contours were extracted from the binary images and plotted in Celltool [9], an open source software, to simulate the motion of the cells/fragments over time. For principle component analysis, polygons were extracted from a large population of cell images and mutually aligned. Principal modes of shape variation were determined by principal component analysis of the population of polygonal cell outlines, and scaled in terms of the standard deviation of the population for each mode of variation, which was detailed previously [10].

Fluorescence labeling: Trypsinized cells were seeded in glass bottom plates. Fragments were induced with 100 nM Staurosporin for 30 minutes at 35^{o}C. Samples were fixed in 4% paraformaldehyde and permeabilized with 0.5% Triton X-100 in Phosphate buffered saline (PBS). All dyes were purchased from Invitrogen and used per manufacturer's instructions. The Golgi body was labeled with 10 μg/ml wheat germ agglutinin (WGA) conjugated with Alexa Fluor 594. Actin was stained with 5 μg/ml Phalloidin conjugated with Alexa Fluor 488 and the nucleus was stained with 2 μg/ml Hoechst 33342. The Endoplasmic Reticulum (ER) of live cells was labeled with 1 μM ER-Tracker Red (glibenclamide BODIPY TR). Staining was performed in Hank's Balanced Salt Solution (HBSS) with calcium and magnesium (116.5mM NaCl, 5.4mM KCl, 0.25mM Na2HPO4, 0.44mM KH2PO4, 1.3mM CaCl2, 1mM MgSO4, 4.2mM NaHCO3). Cells were incubated at room temperature with the staining buffer for 30 min. After washing with fresh medium, fragments were induced by staurosporine treatment. Images were taken in a Zeiss Axio-Observer inverted microscope equipped with a CoolSnap HQ2 CCD camera (Photometrics) using a 63x objective (NA=1.4) and 1.6 optovar.

Statistics: All experiments were repeated and produced similar results. In most cases a representative experiment is shown, unless stated otherwise. Data are presented as means ± standard error. In order to conclude the size dependency a correlation coefficient corresponding to the directedness were calculated. To compare group differences (EF *vs* no EF or drug treatment *vs* no treatment) either chi-squared test or paired/unpaired, two-tailed Student's *t*-test were used. A *P* value less than 0.05 is considered as significant.

Supplemental References

1. Ofer, N., Mogilner, A., and Keren, K. (2011). Actin disassembly clock determines shape and speed of lamellipodial fragments. Proceedings of the National Academy of Sciences of the United States of America *108*, 20394-20399.
2. Zhao, M., Agius-Fernandez, A., Forrester, J.V., and McCaig, C.D. (1996). Directed migration of corneal epithelial sheets in physiological electric fields. Invest Ophthalmol Vis Sci *37*, 2548-2558.
3. Song, B., Gu, Y., Pu, J., Reid, B., Zhao, Z., and Zhao, M. (2007). Application of direct current electric fields to cells and tissues in vitro and modulation of wound electric field in vivo. Nat Protoc *2*, 1479-1489.
4. Sun, Y.H., Reid, B., Fontaine, J.H., Miller, L.A., Hyde, D.M., Mogilner, A., and Zhao, M. (2011). Airway Epithelial Wounds in Rhesus Monkey Generate Ionic Currents That Guide Cell Migration to Promote Healing. J Appl Physiol.
5. Allen, e.a. (2012). Electrophoresis of cellular membrane components creates the directional cue guiding galvanotaxis.
6. Tai, G., Reid, B., Cao, L., and Zhao, M. (2009). Electrotaxis and wound healing: experimental methods to study electric fields as a directional signal for cell migration. Methods Mol Biol *571*, 77-97.
7. Gruler, H., and Nuccitelli, R. (1991). Neural crest cell galvanotaxis: new data and a novel approach to the analysis of both galvanotaxis and chemotaxis. Cell Motil Cytoskeleton *19*, 121-133.
8. Otsu, N. (1979). A threshold selection method from gray-level histograms. IEEE Transactions on Systems, Man and Cybernetics *9*, 62-66.
9. Pincus, Z., and Theriot, J.A. (2007). Comparison of quantitative methods for cell-shape analysis. J Microsc *227*, 140-156.
10. Barnhart, E.L., Lee, K.C., Keren, K., Mogilner, A., and Theriot, J.A. (2011). An adhesion-dependent switch between mechanisms that determine motile cell shape. PLoS biology *9*, e1001059.